Journal of Inorganic Biochemistry xxx (2015) xxx–xxx

Contents lists available at ScienceDirect

Journal of Inorganic Biochemistry

journal homepage: www.elsevier.com/locate/jinorgbio

The effect of phosphate on the nuclease activity of vanadium compounds

Nataliya Butenko [a,b], José Paulo Pinheiro [a], José Paulo Da Silva [a], Ana Isabel Tomaz [b,c], Isabel Correia [b], Vera Ribeiro [d], João Costa Pessoa [b], Isabel Cavaco [a,b,*]

[a] Departamento de Química e Farmácia, Universidade do Algarve, Campus de Gambelas, 8005-139 Faro, Portugal
[b] Centro de Química Estrutural, Instituto Superior Técnico, Universidade de Lisboa, Av Rovisco Pais, 1049-001 Lisboa, Portugal
[c] Faculdade de Ciências da Universidade de Lisboa, Campo Grande, Lisboa, Portugal
[d] Centro de Biomedicina Molecular e Estrutural, Universidade do Algarve, Campus de Gambelas, 8005-139 Faro, Portugal

ARTICLE INFO

Article history:
Received 1 December 2014
Received in revised form 16 April 2015
Accepted 16 April 2015
Available online xxxx

Keywords:
Inorganic nucleases
DNA cleavage
Vanadium acetylacetonate
Oxidovanadium(IV/V) complexes
Phosphate

ABSTRACT

The nuclease activity of $VO(acac)_2$ (**1**, acac = acetylacetone) and its derivatives $VO(hd)_2$ (**2**, hd = 3,5-heptanedione), $VO(Cl\text{-}acac)_2$ (**3**, Cl-acac = 3-chloro-2,4-pentanedione), $VO(Et\text{-}acac)_2$ (**4**, Et-acac = 3-ethyl-2,4-pentanedione) and $VO(Me\text{-}acac)_2$ (**5**, Me-acac = 3-methyl-2,4-pentanedione), is studied by agarose gel electrophoresis, UV–visible spectroscopy, cyclic and square wave voltammetry and ^{51}V NMR. The mechanism is shown to be oxidative and associated with the formation of reactive oxygen species (ROS). Hydrolytic cleavage of the phosphodiester bond is also promoted by **1**, but at much slower rate which cannot compete with the oxidative mechanism. The generation of ROS is much higher in the presence of phosphate buffer when compared with organic buffers and this was attributed to the formation of a mixed-ligand complex containing phosphate, $(V^{IV}O)(V^{V}O)(acac)_2(H_nPO_4^{n-3})$, presenting a quasi-reversible voltammetric behavior. The formation of this species was further observed by Electrospray Ionization Mass Spectrometry (ESI-MS). Phosphate being an essential species in most biological media, the importance of the formation of mixed-ligand species in other vanadium systems is emphasized.

1. Introduction

Designing metal complexes that can cleave DNA – inorganic nucleases – is a field of numerous applications, from cancer therapy to DNA manipulation. Some vanadium complexes (VCs), in particular derivatives of oxidovanadium(IV) acetylacetonate, $V^{IV}O(acac)_2$, have been shown to be very efficient inorganic nucleases [1]. $V^{IV}O(acac)_2$ and other VCs have also been extensively studied as potential drugs for the treatment of diabetes mellitus and other diseases [2–6].

The aqueous chemistry of VCs can be very complex particularly in dilute solutions. When dissolved in water a VC can form a variety of different species, which may be essentially different from the original compound. In biological fluids such speciation may be more complex. Identifying the species responsible for DNA cleavage is important both to design more efficient nucleases and to assess eventual toxicity of these compounds. Speciation studies of VCs are typically done at millimolar concentration levels [7–11], much higher than the metal concentrations relevant in biological systems, which are in the micromolar or nanomolar range. The speciation of VCs at such low concentrations is not well known or understood, as they are below the detection limits of the most common analytical techniques in metal analysis such as EPR, NMR, UV–visible (UV–Vis) absorption spectroscopy, circular dichroism and potentiometry.

Phosphate is an important biogenic ligand and one of the relevant constituents of human serum and interstitial fluids. It is involved in an extensive number of biological recognition and bio-catalytic systems [6,12–14]. Its concentration in blood is approximately 1.1 mM [15,16], whereas in working muscle cells it can be as high as 40 mM [17]. In spite of being a weak coordinating ligand, when metal complexes are in the micromolar range of concentration, the phosphate ligand-to-metal ratio can be as high as 20,000. The formation of phosphate complexes and mixed-ligand complexes containing phosphate and the original ligand cannot be overlooked.

The few studies conducted on the speciation of vanadium with phosphate were carried out by the groups of L. Pettersson and T. Kiss. Pettersson et al. studied the speciation of vanadates and H_2O_2 in the presence of phosphate and concluded that peroxovanadate-phosphate complexes are not likely to be formed under human physiological conditions [18]. Kiss et al. determined that ternary complexes with phosphate may be formed in blood at neutral pH with maltonate-, picolinate- and methylpicolinate-$V^{IV}O$-systems [8,9].

When studying the nuclease activity of several VCs, we found that not only $V^{IV}O(acac)_2$ was surprisingly active [19], but also that its activity was much higher in phosphate than in the presence of other buffers. This was attributed to the formation of mixed complexes of phosphate and acac and also to a scavenger effect of organic buffers that masks nuclease activity by radicals.

* Corresponding author at: Departamento de Química e Farmácia, Universidade do Algarve, Campus de Gambelas, 8005-139 Faro, Portugal.
E-mail address: icavaco@ualg.pt (I. Cavaco).

http://dx.doi.org/10.1016/j.jinorgbio.2015.04.010
0162-0134/

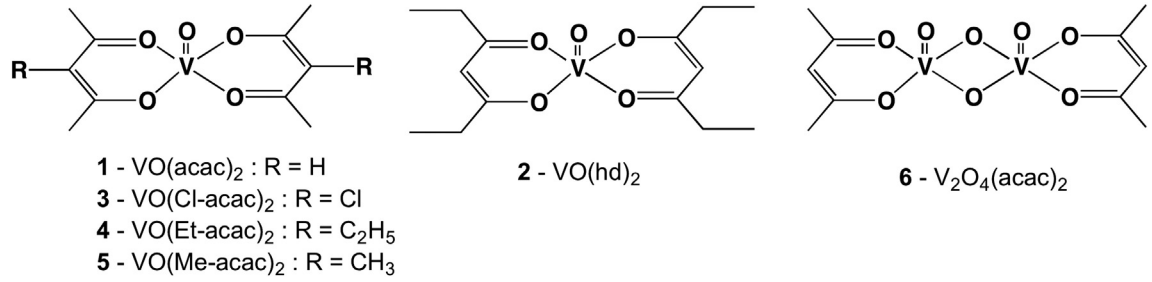

Fig. 1. Proposed structural formulae of complexes **1**–**6**.

The aim of the present work is to understand the nature of DNA cleavage by $V^{IV}O(acac)_2$ derivatives and the role of phosphate in this interaction. Derivatives of $V^{IV}O(acac)_2$ were prepared containing side groups of different nucleophilicity and with different metal oxidation states. Their nuclease activity was assessed by agarose gel electrophoresis (AGE), while solution speciation was evaluated by UV–Vis absorption spectroscopy, ^{51}V NMR spectroscopy, cyclic voltammetry and square wave voltammetry. The nature of the DNA cleavage mechanism – radical or hydrolytic – was assessed by NMR spectroscopy and by spectrofluorometry using well-known probes for this type of reactions.

The complexes studied were $V^{IV}O(acac)_2$ (1, acac = 2,4-pentanedione, also called acetylacetone), $V^{IV}O(hd)_2$ (2, hd = 3,5-heptanedione), $V^{IV}O(Cl\text{-}acac)_2$ (3, Cl-acac = 3-chloro-2,4-pentanedione), $V^{IV}O(Et\text{-}acac)_2$ (4, Et-acac = 3-ethyl-2,4-pentanedione) and $V^{IV}O(Me\text{-}acac)_2$ (5, Me-acac = 3-methyl-2,4-pentanedione). The methyl-, ethyl- and chlorine-groups in 3–5 are substituents of atom C3 of acac and are expected to affect the redox behavior of these complexes. The DNA cleavage activity of a dioxidovanadium(V) complex with acac, $V^{V}{}_2O_4(acac)_2$ (6) and oxidovanadium(IV) sulfate (7) were also studied. The proposed structural formulae of complexes 1–6 are represented in Fig. 1.

2. Experimental

2.1. Materials

All solutions were prepared with Millipore® water of maximum conductivity 0.054 μS/cm. All chemicals used were of analytical grade. $V^{IV}O(acac)_2$ (**1**), $VOSO_4$ (**7**), Hd, Cl-acac, Et-acac, Me-acac, ethidium bromide, trizma® base (≥99.9%), phosphate buffered saline tablets (PBS),[1] agarose powder (type I, low electoendoosmosis), ethidium bromide (EtBr), terephthalate (disodium salt, 98%), 4-nitrophenyl phosphate disodium salt hexahydrate (NPP) and bis-*p*-nitrophenyl phosphate sodium salt (BNPP) were supplied by Sigma-Aldrich; 3-(N-morpholino)propanesulfonic acid (MOPS, 99.5%) was from Fluka; di-potassium hydrogen phosphate (99%) and hydrogen peroxide (30% w/v) were from Panreac; mercaptopropionic acid (MPA, >99%) and potassium peroxomonosulfate (oxone, min 4.5% active oxygen) were purchased from Acros; acetylacetone (99.5%), titriPUR® sodium hydroxide solution and suprapur® and nitric acid (65%) were Merck products; ammonium-*meta*-vanadate was from Riedel-de Haën. Phosphate, HEPES and MOPS buffers (100 mM) were prepared by adjusting the pH to 7.0–7.4 with nitric acid or sodium hydroxide.

Stock solutions of VCs were freshly prepared by dissolving an exact (±0.5 mg) mass of the compound in 200 mL of water or buffer to obtain ~200 μM solution. The natural uncertainty coming from this procedure is ca. 10%. Complex **3** is poorly soluble in water (≪50 μM at room temperature), hence its concentration was unknown. Instead, a saturated solution of **3** was used and diluted to 1:2 and 1:4 to check for concentration effect on nuclease activity. The common procedure of dissolving the complexes in DMSO and diluting with water was not used as DMSO would interfere as a radical scavenger.

2.2. Synthesis

$V^{IV}O(acac)_2$ (**1**), is commercially available and was used as received. Complexes **2**, **4** and **5** were obtained by reaction of $V^{IV}OSO_4$ with an excess of the ligands as previously described [20,21]. Complex **3** was synthesized for the first time following the same procedure. Complex **6** was prepared according to the literature [22]. Fourier transform (FT)-IR spectra in the range 4000–400 cm^{-1} were recorded on a Jasco FT/IR-4100 spectrometer using KBr pellets.

$V^{IV}O(hd)_2$ (**2**): dark green solid; 74.7% yield; elemental analysis (%) calculated for $[VO(C_7H_{11}O_2)_2]\cdot 0.25H_2O$ (found): C 51.62 (51.52); H 6.96 (7.16). IR (KBr, cm^{-1}): 2976, 1552, 1534, 1411, 1371, 1311, 1248, 1186, 1170, 1076, 1000, 991, 954, 861, 810, 779.

$V^{IV}O(Cl\text{-}acac)_2$ (**3**): light green solid; 91.6% yield; elemental analysis (%) calculated for $[VO(C_5H_6O_2Cl)_2]$ (found): C 35.96 (36.01); H 3.62 (3.48). IR (KBr, cm^{-1}): 3001, 2972, 2930, 1576, 1464, 1424, 1374, 1352, 1298, 1049, 1024, 1015, 905, 703, 638, 617, 509, 469, 451.

$V^{IV}O(Et\text{-}acac)_2$ (**4**): green solid; 54% yield; elemental analysis (%): calculated for $[VO(C_7H_{11}O_2)_2]$ (found): C 52.34 (52.19); H 6.90 (7.12). IR (KBr, cm^{-1}): 2962, 2874, 1559, 1467, 1454, 1376, 1331, 1296, 1259, 1173, 1066, 1000, 958, 916, 790, 780, 722, 686, 618, 490, 463, 441.

$V^{IV}O(Me\text{-}acac)_2$ (**5**): light green; 70% yield; elemental analysis (%): calculated for $[VO(C_6H_9O_2)_2]$ (found): C 49.16 (49.05); H 6.19 (6.39). IR (KBr, cm^{-1}): 3015, 2926, 1566, 1480, 1428, 1337, 1300, 1177, 997, 981, 898, 733, 660, 619, 490, 468.

$V_2O_4(acac)_2$ (**6**): dark brown solid; 61% yield; elemental analysis (%): calculated for $[V_2O_4(C_5H_7O_2)_2]\cdot 0.25H_2O$ (found): C 30.67 (30.45); H 3.73 (3.85). IR (KBr, cm^{-1}): 3422, 3112, 1580, 1534, 1413, 1384, 1348, 1294, 1283, 1033, 991, 983, 949, 934, 818, 790, 775, 672, 604.

2.3. Nuclease activity

2.3.1. Agarose gel electrophoresis (AGE)

DNA cleavage activity was tested by AGE using plasmid DNA (pDNA). Commercial pDNA contains EDTA and tris, both of which would interfere in this study [1]. As such, a non-commercial pDNA (pA1) was prepared. pA1 consists of a full-length cDNA from Cytochrome P450 CYP3A1 inserted in the PBS plasmid vector (pBluescribe, Stratagene, UK) [23]. The pDNA was amplified in *Escherichia coli* MACH1 and purified using Nucleobond® AX Anion Exchange Columns for quick purification of nucleic acids from MACHEREY-NAGEL. The concentration of pDNA was measured spectrophotometrically at λ = 260 nm. Each reaction mixture was 20 μL containing 6 μL of water, 2 μL of 100 mM stock buffer solution pH 7.0–7.4, 2 μL of pA1 DNA (0.2 μg) and 10 μL of complex (3–100 μM). The [metal]:[DNA(base pair)] ratio (ri) varied from 0.2 to 6.7. Typically, duplicate controls of supercoiled (Sc) and of linear (Lin) form were introduced into the first

[1] PBS is a pH 7.4 phosphate buffered medium with controlled ionic strength: 10 mM phosphate buffer, 2.7 mM KCl, 137 mM NaCl. When used in the form of tablets higher concentration of pH buffer can be prepared as necessary, keeping the same ratio of its components.

Please cite this article as: N. Butenko, et al., The effect of phosphate on the nuclease activity of vanadium compounds, J. Inorg. Biochem. (2015), http://dx.doi.org/10.1016/j.jinorgbio.2015.04.010

and last wells of each gel. The final concentration of buffers (K_2HPO_4/HNO_3, MOPS/NaOH or HEPES/NaOH) was 10 mM, unless indicated otherwise. In experiments with activating agents or radical scavengers, these were added prior to the addition of complexes. The final concentration of reductant (MPA, mercaptopropionic acid) and oxidant (oxone, $KHSO_5$) was 200 μM, while that of radical scavengers was 40 mM. The electrophoresis was carried out as described in [1].

Bands were visualized and photographed using an AlphaImager from Alpha Innotech. Peak areas of each DNA form were measured by densitometry using AlphaEaseFC™ software (Alpha Innotech). Due to a low binding affinity of ethidium bromide for the supercoiled DNA form, the measured areas of the Sc DNA form were multiplied by a factor of 1.47 [24]. Then, the percentage of each DNA form was calculated. The cleavage efficiency was evaluated by the increase in the amount of nicked DNA (Nck, open circular - form II) and Lin DNA (form III) in relation to the Sc DNA (form I). These changes reflect the ability of metal complexes to promote single and double strand cleavage, respectively.

Experiments under inert atmosphere were carried out using an inert line and Schlenk techniques, where sample eppendorfs were supported inside Schlenk flasks. Samples were incubated under nitrogen for 1 h; the remaining experiment was carried out in air as described above.

Standard deviation for repeatability (s_r)[2] for the peak area within the same gel was estimated as 8%, 6% and 8% for the Sc, Nck and Lin forms, respectively [25].

2.4. Evaluation of the stability of the complexes in aqueous solutions

2.4.1. UV–Vis spectroscopy

Visible absorption spectroscopy was used to ascertain the stability of complexes **1**–**5** and **7** in 10 mM buffered aqueous solutions. UV–Vis spectra were recorded at room temperature on a Hitachi U-2000 double beam spectrometer with 1 or 4 cm path-length quartz cells from 350 to 950 nm. Compounds **2**, **4**, **5** and **7** in 100% PBS (pH 7.4) were of 1.2 mM concentration, **1** and **3** were 2.0 mM in 1 and 100% DMSO, respectively.

2.4.2. Electroanalytical methods

The electrochemical behavior of **1**–**6** was studied by cyclic and square wave voltammetry (CV and SWV) in phosphate and MOPS buffers (10, 30 and 100 mM) using an Eco Chemie Autolab Potentiostat/Galvanostat 12 in conjunction with a Metrohm 663VA stand. A three-electrode configuration was used with a mercury drop working electrode, a saturated calomel (SCE) or an Ag/AgCl 3 M as reference electrode and a Pt wire auxiliary electrode. CV was carried out at 50 mV/s scan rate and SWV at 25 Hz. High-purity N_2 gas was used to purge solutions prior to each measurement for at least 15 min and between scans for 1 min. During all measurements a continuous flow of nitrogen was passing above the solution to ensure removal of dissolved oxygen. The scans of buffer solutions with no complex were considered as blank voltammograms. Complex concentrations were similar to those used in digestion with pDNA, i.e., 2, 5, 10, 20 and 50 μM.

In experiments increasing the concentration of phosphate buffer from 1 to 20 mM, the measurement started by running the scan of 1 mM buffer (blank), followed by addition of **1** to have a concentration of 50 μM. The experiment continued with gradual additions of buffer (100 mM) to 25 mL of solution increasing the buffer concentration to 2, 4, 6, 10 and 20 mM. The solution volume at the end of the experiment was 30 mL, corresponding to a maximum dilution of the VC of 20%. Similar procedures were followed when increasing the concentration of phosphate in the presence of MOPS buffer and vice versa.

[2] S_r measures the random variability within each experiment. S_r values were estimated from analysis of variance (single factor ANOVA) of duplicates from 11 different runs. S_r for the peak area was estimated from duplicates of pDNA (not incubated). S_r for the whole procedure was estimated from duplicates of samples incubated with metal complexes.

Peak potentials and peak currents were determined from the experimental scans by the General Purpose Electrochemical Chemistry software (GPES, version 4.9, Eco Chemie B.V. Utrecht, Netherlands).

2.4.3. Electrospray ionization mass spectrometry (ESI-MS)

ESI-MS spectra were obtained on a Bruker Daltonics HCT ultra mass spectrometer (ion trap), equipped with an ESI source (Agilent) using a nickel-coated glass capillary (inner diameter of 0.6 mm). The ions were continuously generated by infusing the aqueous sample solution (4 $\mu L/min^{-1}$) into the source with the help of a syringe pump (KdScientific, model 781100, USA). The solutions were studied in the negative and positive polarities. Typical conditions for the positive polarity were: capillary voltage (CE): −3 kV; capillary exit voltage: 133 V; skimmer voltage: 32 V; drying gas temperature: 300 °C; drying gas flow: 10 L/min; nebulizer gas pressure: 30 psi. The conditions for the negative polarity were: capillary voltage (CE): 3.0 kV; capillary exit voltage: −133 V; skimmer voltage: −32 V; drying gas temperature: 300 °C; drying gas flow: 10 L/min; nebulizer gas pressure: 30 psi.

2.4.3.1. Solution preparation. The ESI-MS measurements were carried out for freshly prepared solutions of **1** or **7** in MilliQ® water, MOPS or phosphate buffer. Complex concentrations were 10, 50 and 100 μM in 0, 10 or 100 μM of buffers. All solutions of **1** buffered with phosphate or MOPS buffer had pH 6.8–6.9. After one day the pH of the solutions containing 100 μM of VC and 10 μM of buffer had decreased to 4.7–5.4. The pH of freshly prepared **1** in H_2O was 5.4 and after one day it decreased to 4.7.

2.5. Mechanistic studies

2.5.1. Fluorescence spectroscopy

Terephthalic acid (TPA, non-fluorescent) was used to trap hydroxyl radicals [26] forming 2-hydroxy-terephthalic acid (HTPA, fluorescent), which was then measured by spectrofluorometry. Stock solutions of 400 μM TPA in buffer (solution A) and VC **1**, **4** and **7** 125 μM in water (solution B) were prepared. TPA was dissolved in phosphate, in MOPS or in a mixture of the two buffers (pH 7.4). Warming the solutions to ~80 °C in a water bath was necessary to ensure the dissolution of TPA. Typically, 10 mL of solution A were mixed with 8 mL of solution B and 2 mL of water or 30% H_2O_2. Blank samples were 200 μM solutions of TPA in phosphate or MOPS buffer. All solutions were kept at room temperature between the measurements. Spectra were recorded on a FluoroMax®-3 spectrometer in a 3-cm quartz rectangular spectrofluorometer cuvette. Excitation spectra were obtained in the range of 250–400 nm with emission at 435 nm and emission spectra in the range of 350–500 nm with excitation at 323 nm. Slit width and scan rate were 1 nm (excitation and emission) and 1 nm/s.

2.5.2. NMR studies

Hydrolysis of nitrophenyl phosphate (NPP) and bis-4-nitrophenyl phosphate (BNPP) (4 mM) by **1** (sat, C < 3 mM) was followed by ^1H and ^{51}V NMR spectroscopy on a Bruker Avance 400. The acquisition parameters were as follows: 33 KHz spectral width, 25 μs pulse width, 0.5 s acquisition time and 10 Hz line broadening. In order to ensure their buffering power, pH buffer solutions were prepared with concentrations 10× higher that NPP and BNPP, i.e. 40 mM MOPS or PBS, prepared in D_2O (pH 7.2–7.4). ^{51}V and ^1H chemical shifts were referenced relative to neat V^VOCl_3 as the external standard and DSS (4,4-dimethyl-4-silapentano-1-sulfonic acid), respectively. The reaction mixtures were constantly kept at 50 °C and observed during 10 days. The NMR signals were assigned by comparison with literature data [6,27].

Please cite this article as: N. Butenko, et al., The effect of phosphate on the nuclease activity of vanadium compounds, J. Inorg. Biochem. (2015), http://dx.doi.org/10.1016/j.jinorgbio.2015.04.010

3. Results and discussion

3.1. DNA cleavage activity

3.1.1. $V^{IV}O(acac)_2$ derivatives

Nuclease activity can be measured by the extent of the degradation of the Sc into Nck and Lin form after incubation with an inorganic nuclease. Changes in the relative intensities of AGE bands for Sc, Nck and Lin when compared to a control of non-incubated DNA are a good indicator for evaluation of DNA cleavage.

The nature of the buffer was found to play a key role in DNA degradation by oxidovanadium nucleases [1]. Thus, the nuclease activity of $V^{IV}O(acac)_2$ and derivatives was studied in two different buffer media, i.e., inorganic (phosphate) and an organic (MOPS or HEPES) at pH 7.0–7.4.

Fig. 2 compares the activity of **1**–**5** at concentrations 50 and 100 μM (ri 3.3 and 6.7). Complex **1** shows the highest intensities for the Nck and Lin bands and lowest for Sc and as such appears to be the most active nuclease. Complex **2** shows lower nuclease activity. The activity of **3** seems to be similar to that of **1** and **2**, but in fact **3** is poorly soluble in water and its concentration is much lower than those of the other compounds. The experiments were done with a saturated solution of **3** which was diluted 1:2 and 1:4 to concentrations unknown but lower than 50 and 100 μM. Taking this into account, **3** must be considered more active than **1** or **2**. On the other hand, complexes **4** and **5** have much lower activities with practically no linearization even at 100 μM.

Results of the activity of **1**–**5** in MOPS (Fig. S1 in the Supplementary Materials) agree with previous findings showing much lower nuclease activity of VCs in organic buffers than in phosphate [1]. No linearization of DNA is observed. Nevertheless all complexes promote single-strand cleavage at 50 μM (ri 3.3). The order of decreasing activity can be established as: **1**>**2**>**4**>**5**–**7**. Compound **3** seems to be less active than **4** but in fact, taking into account its low concentration it is probably the most active complex.

$V^{IV}O(acac)_2$ and derivatives promote the DNA cleavage with different efficiencies (Fig. S2). Based on AGE data, two types of nucleases, strong and weak, can be distinguished in the oxidovanadium(IV)-acac family. The most active compounds, **1**–**3**, are also the most stable ones towards hydrolysis.

3.1.2. $V^{IV}OSO_4$

Controls for the nuclease activity of the $V^{IV}O^{2+}$ aquocomplex consisted in solutions of $V^{IV}OSO_4$ (**7**) and of $V^{IV}O(ClO_4)_2$. Although **7** is commonly reported as an inactive nuclease [19,28], we have observed an irreproducible behavior, i.e., it can show activity as high as that of **1** in some assays, or no activity in others. This lack of reproducibility may be explained since, depending on the concentration used, $V^{IV}O^{2+}$ will hydrolyze and partly precipitate as $V^{IV}O(OH)_2$, especially at neutral pH, or oxidize to V^{V} species [29,30]. Also, the kinetics of the precipitation and oxidation is likely to depend on factors such as the temperature and the process of mixing the solutions, which were not specifically controlled in these experiments. The absence of nuclease activity observed in some tests may be due to extensive precipitation of $V^{IV}O(OH)_2$. When this precipitation is slower or not so extensive, nuclease activity can be observed (Fig. S3). The activity is much stronger in the presence of phosphate buffer than in HEPES. Some activity can be observed under inert atmosphere (Figs. S4 and S5).

3.1.3. V(V) derivatives

Complex **6** was prepared as a model of a possible product or intermediate of the decomposition of **1**. It is poorly soluble in PBS and the ^{51}V NMR spectrum shows only peaks assigned to mono, di and decavanadates. It does not cleave pDNA except in the presence of oxone. This behavior is similar to that of monovanadate(V) [1] and consistent with ^{51}V NMR spectra showing decomposition of the complex into V^{V}-anions upon dissolution.

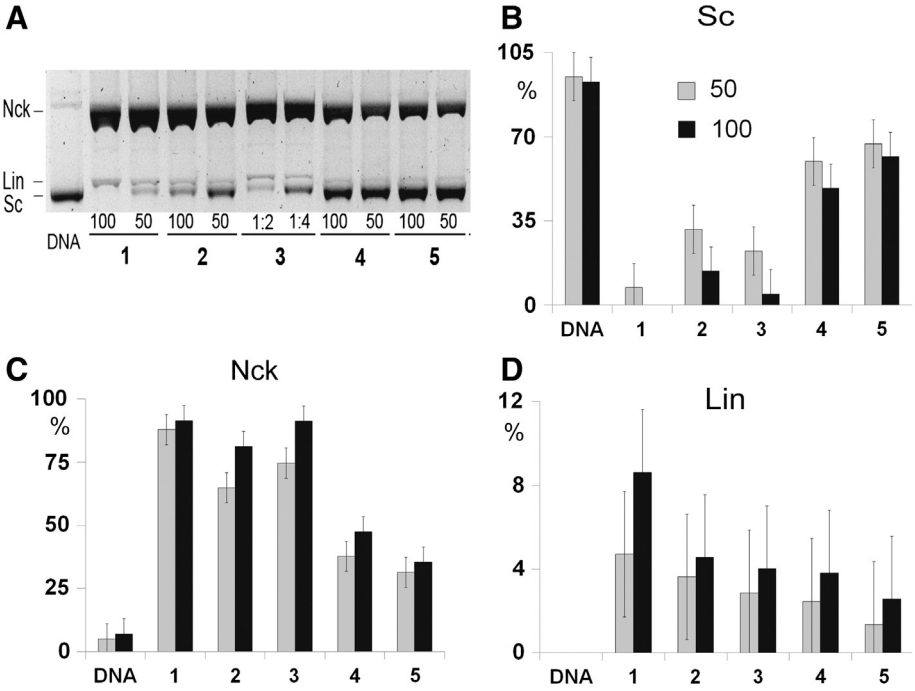

Fig. 2. Nuclease activity of **1**–**5** in PBS buffer. Concentrations are 100 and 50 μM (ri 6.7 and 3.3) except for **3** which was diluted 1:2 and 1:4 from a saturated solution. A: AGE image. B, C, D: percentages of Sc, Nck and Lin forms found by densitometry. "DNA" — control for native DNA. Error bars represent S_r.

Please cite this article as: N. Butenko, et al., The effect of phosphate on the nuclease activity of vanadium compounds, J. Inorg. Biochem. (2015), http://dx.doi.org/10.1016/j.jinorgbio.2015.04.010

3.2. Solution studies

The stability and solution structure of **1** have been extensively studied [1,5,21,31–35]. The present work further explores the stability of VCs **1**–**5** in aqueous solution at neutral pH in the presence of different buffers.

3.2.1. UV–Vis spectroscopy studies

Band assignment of the measured UV–Vis spectra (Table S1) was done according to the simplified model of molecular orbital treatment proposed by Ballhausen and Gray for the $[V^{IV}O(H_2O)_5]^{2+}$ [29,36]. The time evolution of the electronic spectra of complexes **1**–**3** shows small changes within 24 h, while the spectra of **5**, **6** and **7** change significantly in less than 2 h, indicating fast hydrolysis of the complexes (Figs. S6 and S7).

A few differences can be found in the spectra obtained in the presence of different buffers, suggesting that there is interaction of constituents of the buffer with the metal complexes. The spectrum of **1** freshly dissolved in HEPES buffer depicts the bands characteristic of a $V^{IV}O$-complex, i.e., 820 nm (band I), 565 nm (band II) and 400 nm where band III appears as a shoulder of an intense charge transfer band; the same complex dissolved in phosphate buffer shows a very similar spectrum. However, when comparing the normalized spectra (Fig. 3) differences become clear. The relative intensity of band I decreases to some extent in phosphate buffer and band II has a small bathochromic shift. The spectra of complex **2** in both buffers show a clearer bathochromic shift in bands I and II. These differences may be due to the change in solvent polarity in different buffers and not to complexation by molecules of the buffer. Evolution with time in both buffers (Fig. 4) shows a slight decrease in intensity in the absorbance spectra, but no change in the position of the bands, suggesting a slow oxidation of the V^{IV} complex into V^{V}. The largest transformation seems to take place in HEPES buffer after 24 h, with an increasing predominance of the charge transfer band close to 350 nm. In PBS buffer, the changes are observed in the band II (at ca. 570 nm) which decreases similarly for **1** and **2**. These findings are in agreement with previous studies showing that **1** is quite stable in aqueous solution at neutral pH [5,21,37]. Surprisingly, ^{51}V NMR spectrum of **1** freshly dissolved in PBS shows the presence of V1, V2 and V4 peaks (Fig. S8), suggesting either a fast partial oxidation and hydrolysis of the complex, or the presence of small contaminants of V(V) in the solid complex.

Compound **1** is more stable than **2** in aqueous solution regardless of the buffer (Fig. S6), but both complexes are significantly more stable than **4** and **5** (Fig. S7). When **4** and **5** are dissolved in HEPES the absorption bands in the visible region are flattened, indicating fast hydrolysis and oxidation. In the presence of phosphate the spectra show weak bands in the visible range, with band II well defined at 595 nm and band I apparently very weak and with a λ_{max} above 950 nm. These bands are flattened with time confirming hydrolysis and oxidation also in phosphate. Vanadyl sulfate also depicts a similar fast hydrolysis.

All compounds **1**–**7** seem to be more stable in the presence of phosphate than in HEPES. Complexes **4**, **5** and **7** present differences in the relative intensity of the bands in phosphate when compared to **1** and **2** (Fig. 5).

3.2.2. Voltammetry

The stability and electrochemical behavior of complexes **1**–**5** and **7** in aqueous solutions were studied at micromolar concentrations using CV and SWV. To our knowledge, these are the first studies assessing the speciation of VCs in aqueous solutions at low micromolar concentrations.

At the 5, 10 and 20 μM complex concentrations in 100 mM of buffer the CV presents a striking pattern that differentiates the group of complexes with stronger nuclease activity (**1**–**3**) from the weaker ones (**4** and **5**) (Fig. 6, Figs. S9 and S10). In the presence of phosphate buffer the first group of complexes exhibits a quasi-reversible one electron response, with very similar CV. Even though complex **3** did not dissolve completely, it exhibited a clear pattern, similar to **1** and **2**. The cathodic peaks appear at −0.182, −0.186 and −0.186 V for **1**, **2** and **3**, respectively, corresponding to $V^{V} \rightarrow V^{IV}$ reduction and the anodic peaks at −0.060, −0.072 and −0.072 V. The difference (ΔE) between the two peaks for an ideal reversible redox couple at 25 °C would be ΔE = 59 mV/n, where 'n' is the number of electrons exchanged. This difference is 122 mV for **1** and 114 mV for **2** and **3**. The peak intensity ratio is close to 1 and the position of the peaks did not change when the scan ratio varied. This is consistent with a reversible electrochemical reaction involving formation of dinuclear species upon the exchange of one electron:

$$\left(V^{V}O\right)_2(acac)_2\left(H_nPO_4{}^{n-3}\right) + e^- \rightleftharpoons \left(V^{V}O\right)\left(V^{IV}O\right)(acac)_2\left(H_nPO_4{}^{n-3}\right)^- \quad (1)$$

However, such behavior is not observed in the presence of an organic buffer. The CV of the same complexes in MOPS (Figs. 6 and S9) shows irreversible behavior and weaker signals suggesting the formation of a mixture of species.

The CV of **7** (Fig. S10), in the same conditions, shows a similar pattern; however, the cathodic peak is at a less negative potential, −0.156 V (vs. SCE), while the anodic peak maintains a position close to −0.065 V. This suggests that the redox pair formed when dissolving **1**, **2** or **3** in phosphate buffer differs from the one obtained when dissolving **7**. The difference lies in the stabilization of the reduced form (V^{IV}) by the presence of a bidentate ligand (acac) lowering the reduction potential of the species formed from **1** and **2** to more negative values. Phosphate, as buffer anion, is a competitor for metal binding sites due to the high ligand to metal ratio (>5000) and may displace the acac molecules in the physiological pH range [9]. However, apparently it does not remove completely the acac ligands in the case of **1**–**3**. It is probable that

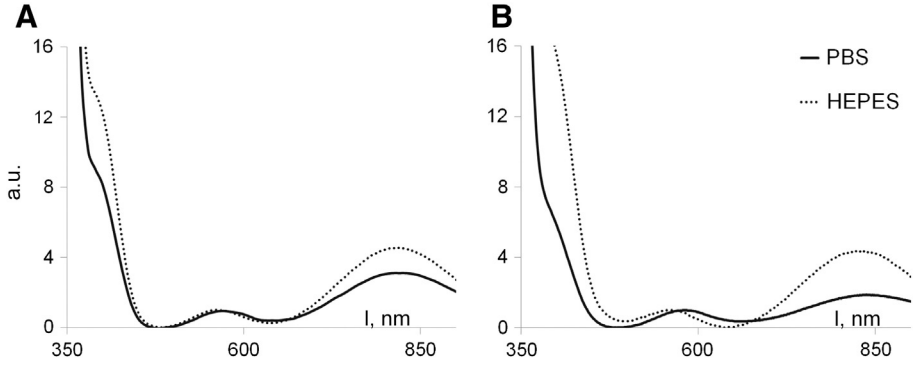

Fig. 3. Absorption spectra (normalized) of **1** (A) and **2** (B) in phosphate and HEPES buffers. Spectra were normalized to show the same intensity (1.0) at band II (ca. 565 nm).

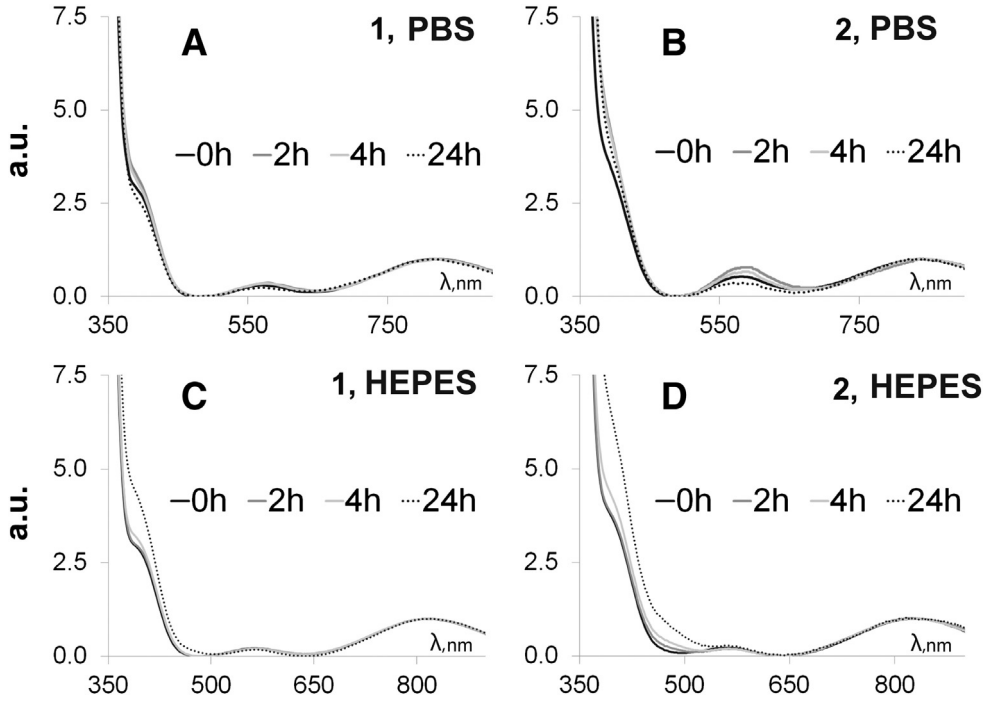

Fig. 4. Absorption spectra (normalized) of **1** and **2** in PBS and HEPES buffers with time. A: **1** in PBS; B: **2** in PBS; C: **1** in HEPES; D: **2** in HEPES. Spectra were normalized to show the same intensity (1.0) at band I (ca. 800 nm).

these complexes equilibrate with phosphate ions to form mixed-ligand species $V^{IV/V}O(acac)(H_nPO_4^{n-3})$.

Complexes **4** and **5** in phosphate buffer present sharp cathodic peaks characteristic of adsorption at the surface of the working electrode. Adsorption significantly affects the electrochemical response resulting in CV of irreversible pattern [38], indicating the formation of species with hydrophobic character.

Consecutive scans of **4** show a clear adsorption anodic peak with increasing intensity and a shift of potential Ep_a from −0.085 V to −0.075 V. The desorption cathodic peak also shifts from Ep_c ~ −0.175 V to −0.146 V (Fig. 7). This is consistent with the formation of an adsorbed film promoted by the oxidation and its desorption upon reduction: the cathodic peak is sharper than the anodic one, suggesting that it corresponds to the desorption process.

Direct scans start each cycle at +0.05 V decreasing the potential to −0.5 V and then increasing it back to +0.05 V. In each consecutive cycle, the concentration of adsorbed vanadium species in the mercury drop increases, resulting in higher intensity of the cathodic peak.

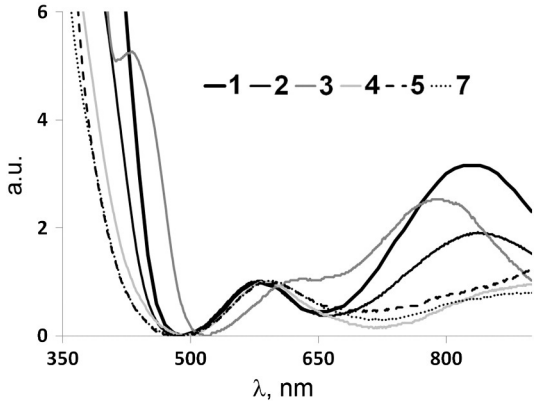

Fig. 5. Absorption spectra (normalized) of **1**–**5** and **7** in PBS. Spectra were normalized to show the same intensity (1.0) at band II (ca. 565 nm).

Reverse scans start at −0.5 V and move to +0.05 V before returning to −0.5 V. The first reverse scan (Fig. 7) shows an oxidation peak at −0.163 V. The subsequent reverse scans are identical to the direct ones. The original anodic peak disapears, giving place to the anodic peak at −0.075 V (also observed in direct scans). This behavior suggests that the anodic peak at −0.075 V is due to a new species formed by the reduction of the adsorbed film. It is not present in the first reverse scan because the adsorbed film, which is formed in the reduction cycle, is not yet there when the first oxidation cycle takes place.

The film formation may be due to polyoxidovanadium species, corresponding to a less soluble hydrophobic structure. Fig. S11 compares the CV of complex **4** with that of a V^V-dinuclear complex of acac, complex **6**. Both show a similar adsorption–desorption pattern. It is reasonable to assume that oxo-bridged V^V-species will form at the high concentrations caused by the adsorption on the surface of the electrode.

In short, in the presence of 100 mM phosphate buffer all studied complexes show relatively simple quasi-reversible redox behavior, involving species containing both the original ligand and phosphate, probably dinuclear species bridged by phosphate. Complexes **4** and **5** show the formation of hydrophobic species upon oxidation, causing different reactions to take place at the electrode surface.

In the presence of MOPS all complexes behave irreversibly and voltammograms show weak and multiple peaks reflecting the formation of multiple electrochemically active species.

Comparison of voltammograms obtained in 100 mM (Fig. 6) and in 10 mM (Fig. S12) phosphate shows that with lower buffer concentration the signal becomes irreversible with more peaks indicating more complex species involved. This suggests that phosphate stabilizes the formed species or, more likely, that phosphate is an important part of the species. On the other hand, results in MOPS show signals as weak and complex in 10 mM as in 100 mM (Figs. S12 and S13).

In comparison to CV, SWV has a much broader dynamic range, higher speed and lower detection limits. SWV analytical determinations can be made at concentrations as low as 10 μM [39]; this allows studying aqueous solutions of VCs at low micromolar concentrations, similar to those used in DNA assays. Fig. 8 compares the results of SWV (direct

Please cite this article as: N. Butenko, et al., The effect of phosphate on the nuclease activity of vanadium compounds, J. Inorg. Biochem. (2015), http://dx.doi.org/10.1016/j.jinorgbio.2015.04.010

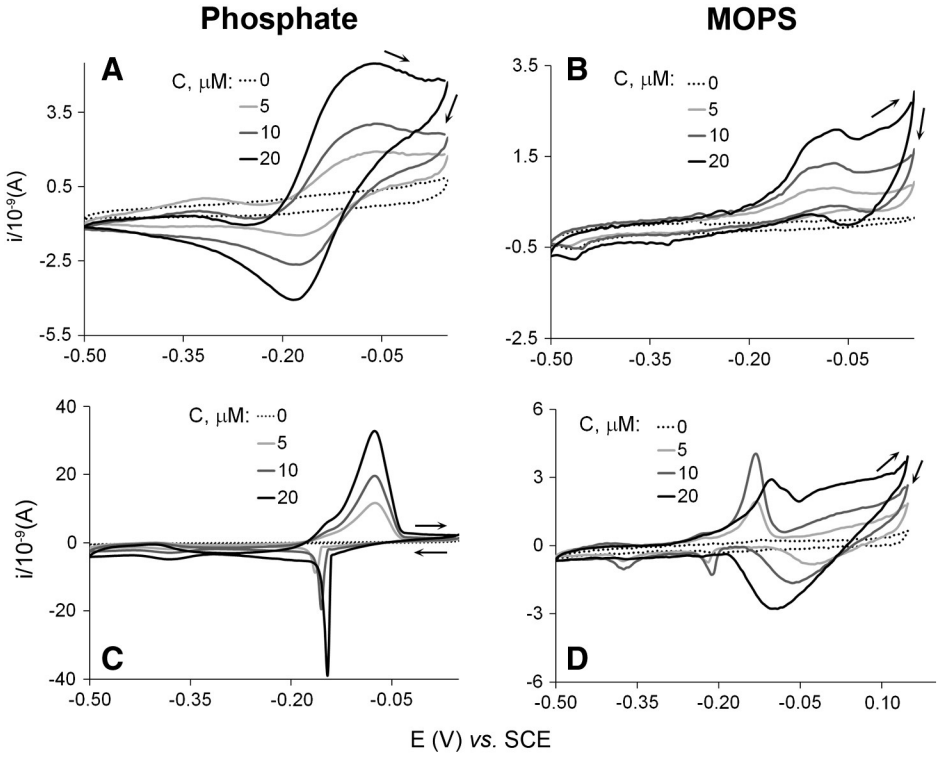

Fig. 6. CV of **1** and **4** (0, 5, 10 and 20 μM) in 100 mM phosphate and MOPS buffers. A: **1** in phosphate; B: **1** in MOPS; C: **4** in phosphate; D: **4** in MOPS.

and reverse), CV and AGE which demostrate the progressive changes with increasing phosphate buffer concentration from 1 to 20 mM. CV is difficult to interpret. SWV indicate the formation of at least two different species which originate the overlapped bands centered at ca. −0.21 (A) and −0.31 V (B) in the SWV reverse (oxidative) scan. Band A disappears with 2 mM of phosphate, while band B increases progressively with increasing buffer concentration, reaching a maximum at ca. 4 mM phosphate. The observed shift of this band to more negative potentials with increasing buffer concentration is due to increasing ionic strength and was not observed in replicate experiments with controlled ionic strength (data not shown). Species causing bands A and B are expected to be mixed ligand complexes $V^{IV}O(acac)_2(H_2PO_4)^-$ (A) and $V^{IV}O(acac)(H_2PO_4)_2^-$ (B). Oxidovanadium phosphate, $VO(H_2PO_4)_2$ (C), is expected to be formed only at higher phosphate concentrations. The AGE experiments (Fig. 8) show that the nuclease activity of **1** is dependent on the phosphate concentration with a maximum at ca. 6 mM of phosphate buffer.

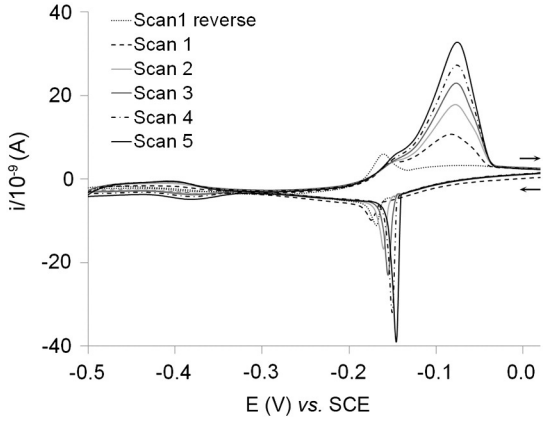

Fig. 7. Consecutive CV scans of 4 at 20 μM in 100 mM phosphate buffer. Five consecutive forward and one reverse scans. The subsequent reverse scans are identical to the displayed direct scans.

The addition of phosphate to a solution of **1** in MOPS (Fig. S14) promotes the formation of species similar to those observed in phosphate buffer. Adding MOPS to a solution of **1** in phosphate does not induce a significant change in the voltammograms, except what is caused by dilution.

3.2.3. ESI-MS

ESI-MS was used to search for structures resulting from the reaction of $V^{IV}O(acac)_2$ and phosphate that could explain the voltammetry and AGE observations. The strong signal quenching effect of the phosphate buffer at mM concentration prevented the analyses of the solutions studied by voltammetry. For this reason, samples of $V^{IV}O(acac)_2$ containing 10 and 100 μM of phosphate were analysed, which are much lower than what is found in biological fluids.

Fig. 9 shows the full scan ESI-MS spectrum of **1** at 10 μM in 100 μM phosphate buffer under positive polarity. The two major signals (m/z 288 and 304) were assigned to $V^{IV}O(acac)_2$. The minor signals were attributed to the expected transformation product $V^{IV}O(acac)^+$ and dinuclear species.

No signals related with products involving phosphate were clearly observed under positive polarity. As products containing the phosphate group can deprotonate, we also analysed the $V^{IV}O(acac)_2$ solutions under negative polarity. The spectrum shows a major peak at m/z 261.8, consistent with a $(V^{IV}O)(acac)(HPO_4)^-$ (Fig. 10). The weaker signal at m/z 426.8 is consistent with $(V^{IV}O)_2(acac)_2(PO_4)^-$.

It should be noted that peaks observed in ESI-MS do not necessarily reflect species existing in solution. Nevertheless, when the presence of the 'same species' is observed both in positive and negative polarity modes it is very likely that they correspond to actual species formed in solution.

Detailed analysis of the positive polarity spectra shows the presence of a few low intensity peaks that, although having intensity very close to

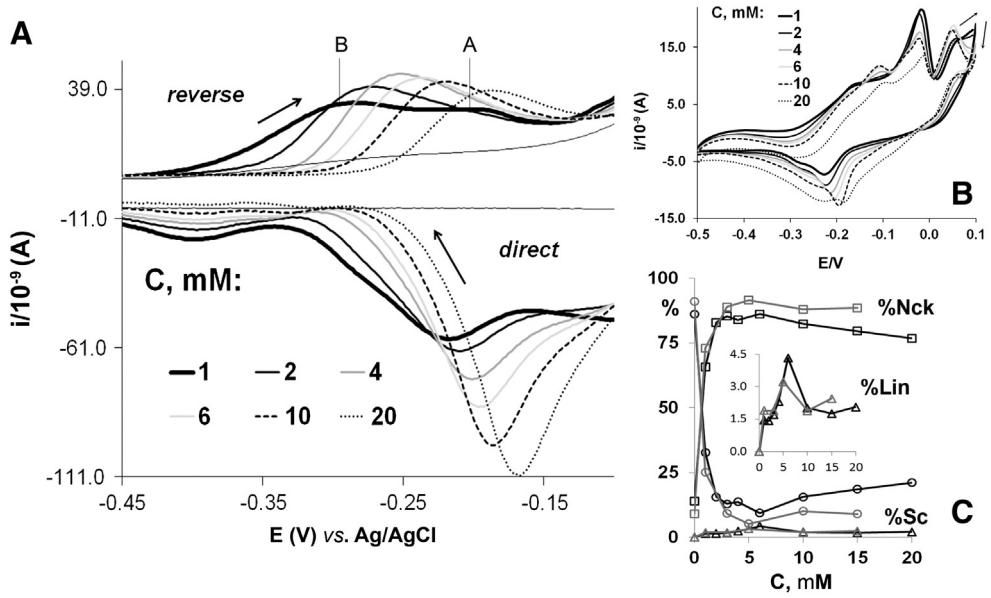

Fig. 8. Electrochemical response and nuclease activity of **1** (20 μM) in increasing concentration of phosphate (1, 2, 4, 6, 10 and 20 mM). A: Direct and reverse SWV. B: CV of the same solution. C: Results of AGE represented as the percentage of Lin DNA form vs. buffer concentration.

the noise level, systematically appear in the same position in replicate experiments and as such cannot be considered random. This is the case of the peaks at m/z 450 and 473 observed in the positive mode. They are tentatively assigned to the dinuclear species containing VO(acac) and phosphate - $(VO)_2(acac)_2(PO_4)$ such as $(V^{IV}O)(V^{V}O)(acac)_2(PO_4).Na^+$ (m/z 450) and $(V^{IV}O)_2(acac)_2(PO_4).2Na^+$ (m/z 473), equivalent to the dinuclear species observed at 426.8 under negative polarity. These peaks are very weak, but reproducible in different experiments (Fig. S15).

3.3. Mechanistic studies

Typically the nuclease activity of metals proceeds either by oxidative or hydrolytic mechanism. It was established that the mechanism of DNA cleavage by **1** is oxidative [1], but the question remained whether a mixed mechanism – both oxidative and hydrolytic takes place.

3.3.1. Radical mechanism

The formation of reactive oxygen species (ROS) in aqueous solutions of the VCs was evaluated by spectrofluorometry through the hydroxylation reaction of TPA to fluorescent HTPA. The use of terephthalate has been extensively reported for the detection of hydroxyl radicals in vitro [40–43] and in vivo studies [44–46]. The reaction is very sensitive and the detection limit of HTPA is 0.5 nM [47].

The hydroxylation of TPA dissolved in phosphate/MOPS buffer in the presence of **1** was followed with time. The fluorescence intensity at 323 nm (excitation spectra) and 435 nm (emission spectra) is interpreted as being proportional to the total number of ROS/hydroxyl radicals formed in solution during the experiment. Although the hydroxylation of TPA by hydroxyl radicals is well studied, no similar reactions of TPA with other agents have been reported. Oxidovanadium(IV) may itself be considered a ROS and it is possible that a species such as a metal complex with the superoxide anion would promote the hydroxylation of TPA without the formation of "free" hydroxyl radicals. For the purpose of this study it is assumed that a ROS capable of promoting the hydroxylation of TPA is damaging to DNA.

In the presence of hydrogen peroxide $V^{IV}O$-complexes are known to produce large amounts of •OH radicals in a Fenton-like reaction. As expected, addition of hydrogen peroxide to solutions of **1** yielded a strong formation of ROS (Fig. S16).

Solutions of **1** showed a slow increase in fluorescence with time, even in the absence of H_2O_2 (Fig. S17). The formation of HTPA in these conditions suggests that $V^{IV}O$-complexes in aqueous solutions generate

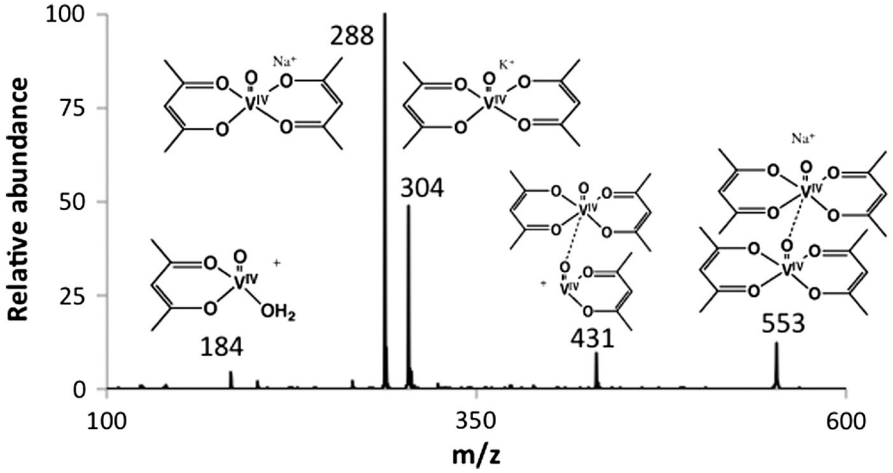

Fig. 9. Full scan ESI-MS spectrum of a 10 μM aqueous solution of **1** in phosphate buffer (100 μM). The insets show tentative assignments of the observed signals.

Please cite this article as: N. Butenko, et al., The effect of phosphate on the nuclease activity of vanadium compounds, J. Inorg. Biochem. (2015), http://dx.doi.org/10.1016/j.jinorgbio.2015.04.010

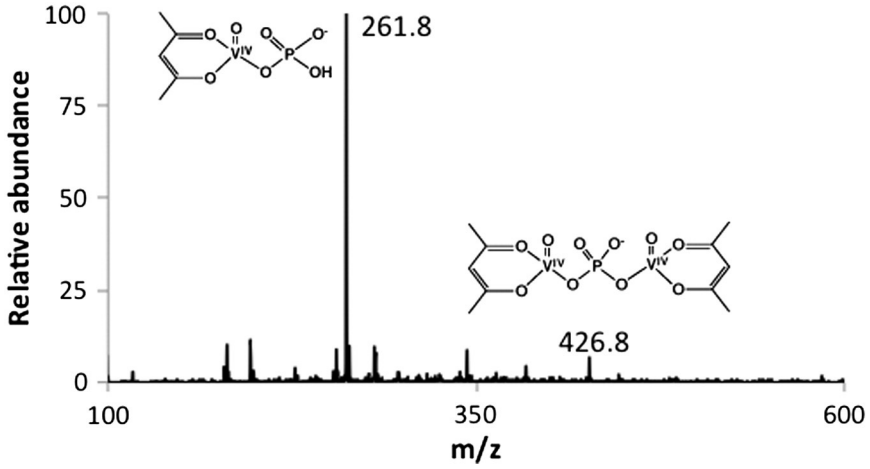

Fig. 10. Full scan ESI-MS spectrum in the negative polarity of a 100 μM aqueous solution of $V^{IV}O(acac)_2$ in phosphate buffer (100 μM). The insets show tentative assignments of the observed signals.

hydroxyl radicals or at least ROS capable of hydroxylating TPA. The reaction was observed both in phosphate and MOPS buffers, but is much faster in the former system. In MOPS a small band was only observed after 25 h of reaction.

The highest fluorescence intensities are observed in phosphate buffer (Fig. S18). The intensity observed for **1** increased with time and stabilized after ca. 20 h, while for **4** the stabilization occurred at a much lower level after 1 h. This is in agreement with the nuclease activity results and corroborates the assumption that the DNA cleavage caused by these complexes follows an oxidative mechanism. Complex **4** is the least active and also shows the lowest fluorescence intensity, therefore it can be assumed that it would generate less ROS capable of hydroxylating TPA and cleaving DNA. Complex **1** is the most active and also generates more ROS. Fluorescence intensities observed in MOPS (Fig. S17) are very low, also reflecting the low nuclease activity observed in organic buffers.

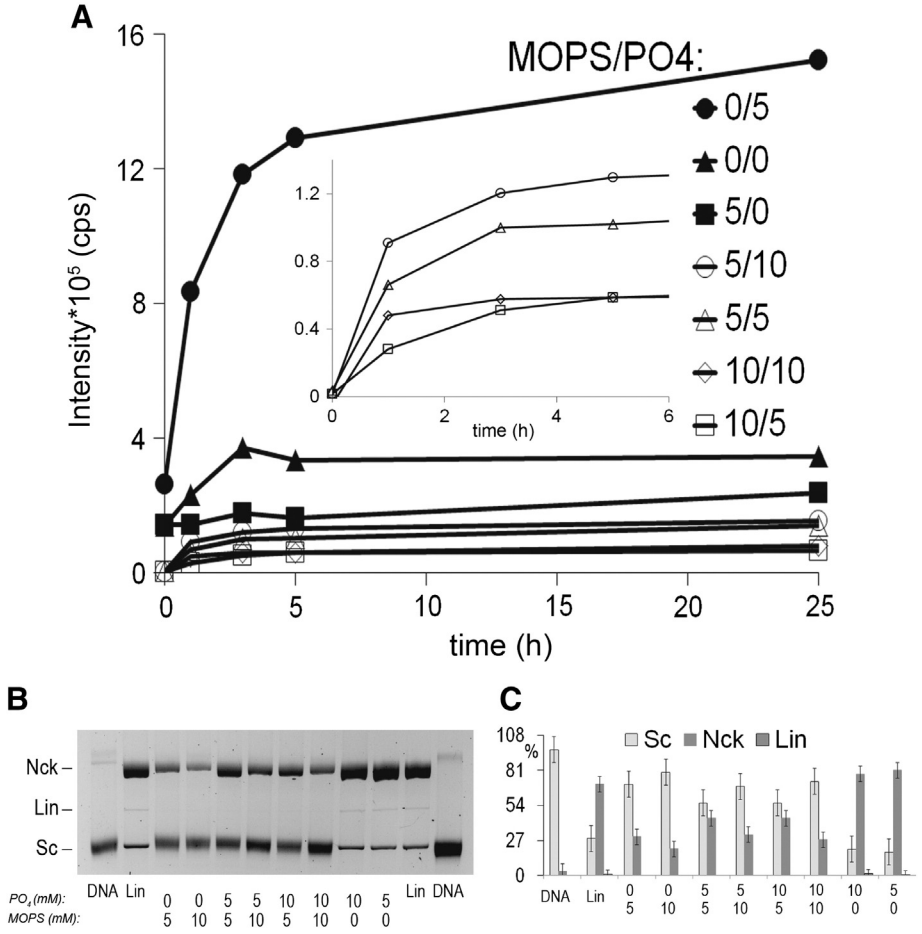

Fig. 11. A: Fluorescence intensity of reaction mixtures with MOPS/phosphate buffer concentration ratios 0/5, 0/0 (unbuffered), 5/0, 5/10, 5/5, 10/10, 10/5. Inset expands the graphic for the first 5 h. B: AGE. "Lin" and "DNA" are the controls for linearized and native DNA. C: Percentage of the DNA forms obtained from densitometry measurements. Error bars represent S_r.

Please cite this article as: N. Butenko, et al., The effect of phosphate on the nuclease activity of vanadium compounds, J. Inorg. Biochem. (2015), http://dx.doi.org/10.1016/j.jinorgbio.2015.04.010

When dissolving TPA and **1** in solutions buffered by mixtures of MOPS and phosphate (Fig. 11), increasing the concentration of phosphate increases the fluorescence intensity when MOPS is kept constant, suggesting that phosphate contributes to the generation of ROS. The most striking result is obtained in the complete absence of MOPS, where fluorescence intensity increases by 10-fold. This can be explained by the scavenging effect of MOPS on "free" radicals [1,48]. Regarding the putative action of ROS, AGE results of DNA cleavage by **1** for the same mixtures of buffers agree with those obtained by fluorescence. The nuclease activity of **1** showed the same pattern, i.e. it was higher in the presence of phosphate and absence of MOPS. When MOPS buffer is not present linearization of DNA is observed; on the contrary, the DNA degradation is always inhibited when MOPS is added. The extent of the inhibition is larger for higher concentrations of MOPS.

The fluorescence results suggest that the tested VCs can generate ROS in neutral aqueous solutions, even in the absence of hydrogen peroxide. These ROS hydroxylate TPA and are probably responsible for the nuclease activity observed for **1** and derivatives. This conclusion can probably be extended to other $V^{IV}O$-complexes that undergo oxidation in biological conditions. We have observed this for **7**, although with low reproducibility due to the precipitation of the hydroxide and oxidation of V^{IV}s.

The generation of ROS by VCs is greatly increased in the presence of phosphate at millimolar concentrations. Rather similar behavior was found for iron: Saran et al. [49] described that the hydroxylation of TPA in aqueous solutions of Fe(II) in the absence of hydrogen peroxide is much more efficient in phosphate buffer. An explanation involved the coordination of phosphate to form a metal-buffer complex inducing the formation of 'non-free' ('crypto') radicals. These were previously discussed by Reinke et al. [50].

The importance of phosphate in the biological chemistry of vanadium is well known [6,11,12,14]. Namely, Liochev et al. [51] addressed the role of phosphate when studying the oxidation of NAD(P)H by vanadate(V), where the nature of the buffer had a significant effect in the outcome of the reaction. They explained it with autoxidation of V^{IV} to V^{V} at neutral pH and the generation of the superoxide anion, which would then be the ROS responsible for the oxidation of NAD(P)H: $V^{IV} + O_2 \leftrightarrows V^{V} + O_2^{-}$. The oxidation of V^{IV} would not normally be complete due to the formation of mixed-valence V^{V}-O-V^{IV} stable polyacids. Phosphate would prevent the formation of these species and, hence, in this buffer the reaction would proceed with much higher generation of superoxide.

The formation of divanadates is usually observed only for vanadium concentrations above 100 μM [52]. At the level of concentration of DNA cleavage experiments of ca. 2–100 μM the proportion of any vanadium(V) polyanion present should be negligible, so Liochev's proposal does not explain the DNA cleavage activity we observed. The formation of V^{V}-phosphate and V^{IV}-phosphate species is well known [12,53], thus it is reasonable to assume that phosphate–oxidovanadium species may form when phosphate is present at buffer concentrations of ca. 10 mM, i.e., with phosphate:metal ratios 100 to 5000. In fact, our results on the electrochemistry of the presently studied systems suggest that this type of species are formed and they have a reversible electrochemical behavior that may facilitate the oxidation of V^{IV} with generation of ROS in neutral aqueous solutions.

3.3.2. Hydrolytic mechanism

The hydrolytic cleavage capability of **1** was studied using two phosphodiester model substrates 4-nitrophenyl phosphate (NPP) and bis-4-nitrophenyl phosphate (BNPP). The reaction mixtures prepared in PBS and MOPS buffers and kept at 50 °C were monitored by ^{1}H and ^{51}V NMR spectroscopy. The results (Fig. S15) show that **1** induces the hydrolytic cleavage of both substrates. The ^{1}H NMR resonances attributed to the product of hydrolysis, NP, are observed after ca. 24 h and increase gradually with time. At ca. 200 h the reaction in PBS seems to be completed as at this point the ^{1}H NMR resonances of the aromatic protons in NPP disappeared (Fig. S19A).

In agreement with the previously reported studies of this reaction [27], the hydrolysis of BNPP into NP is significantly slower than that of NPP.

Monitoring the same reaction mixtures by ^{51}V NMR showed that after 24 h **1** had hydrolysed into inorganic vanadates (Fig. S20). In the same solutions the ^{1}H NMR peaks corresponding to the $V^{IV}O(acac)_2$ complex ('d' in Fig. S19B) disappeared and were replaced by a peak assigned to "free" acac ('e' in Fig. S19B), suggesting that the hydrolysis was complete.

The results show that **1** can promote the hydrolytic cleavage of DNA, but such a reaction is too slow to compete with the oxidative cleavage, which is the predominant mechanism and most likely the only one occurring significantly during 1 h digestion of DNA. It was shown by Steens et al. [27,54] that V^{V}-vanadates can actually promote hydrolytic cleavage of the phosphodiester bond [55] – in particular di- or tetravanadates. It is possible that these are the species responsible for the observed hydrolytic activity in our experiments.

We conclude that $V^{IV}O(acac)_2$ induces the hydrolytic cleavage of the phosphoester bond more efficiently in PBS buffer than in MOPS. The reaction is slow (>24 h at 50 °C) when compared to the oxidative cleavage of pDNA (<1 h at 37 °C). The species responsible for the breakage of the phosphoester bond are probably tetravanadate anions. Therefore, we also conclude that most probably the hydrolytic mechanism does not play an important role in the DNA cleavage activity of $V^{IV}O(acac)_2$.

4. Conclusions and perspectives

It is known that transition metals increase the oxidative stress in cells, which for vanadium has been mainly attributed to the generation of hydroxyl radicals by Fenton-like reactions promoted by physiological hydrogen peroxide.

Our study focused on $V^{IV}O(acac)_2$ but in fact can be applied to other VCs. Oxidative stress due to vanadium has been previously studied in the presence of H_2O_2 but our results show that it may also be important in its absence.

In the presence of phosphate, the metal speciation changes when the buffer concentration varies from 1 to 100 mM. A maximum of nuclease activity is observed for a buffer concentration of ~6 mM when the ratio of phosphate:metal is approximately 100:1. The oxidation of V^{IV} at neutral pH, whether promoted by dissolved oxygen or by water itself, in the presence of phosphate may generate ROS that can hydroxylate TPA and cleave DNA. In the presence of phosphate buffer a mixed-ligand complex is formed which can be oxidized reversibly, allowing the redox reaction to proceed in a catalytic way with a high throughput of ROS capable of cleaving DNA.

A tentative mechanism is proposed (Fig. 12) to account for the behavior of $V^{IV}O(acac)_2$ type complexes observed in this work in the different buffers. The formation of mixed valence dinuclear species $(V^{IV}O)(V^{V}O)(acac)_2(PO_4)$ with a reversible redox behavior justifies the higher oxidative stress observed in phosphate and, hence, the higher nuclease activity. ESI-MS results confirmed the presence of these species in solution.

In the absence of phosphate, the oxidation of V^{IV} generates a complex mixture of species that do not show a reversible redox behavior. It is probable that the generation of ROS is not so intense and, as a result, the extent of the pDNA cleavage decreases.

These results have important implications in the interpretation of the biological activity of VCs. Phosphate is present at variable concentrations – in particular in muscle cells it can vary from 1 to 40 mM and, as emphasized in this work, can enhance the oxidative stress caused by VC. The extent of this effect will depend on the phosphate-metal ratio and is probably caused by mixed-ligand species of type VO-L-phosphate.

The nuclease activity observed for the most active complexes – **1**, **2**, **3** (and also **7**) in phosphate buffer is comparable to, or higher, than that

Please cite this article as: N. Butenko, et al., The effect of phosphate on the nuclease activity of vanadium compounds, J. Inorg. Biochem. (2015), http://dx.doi.org/10.1016/j.jinorgbio.2015.04.010

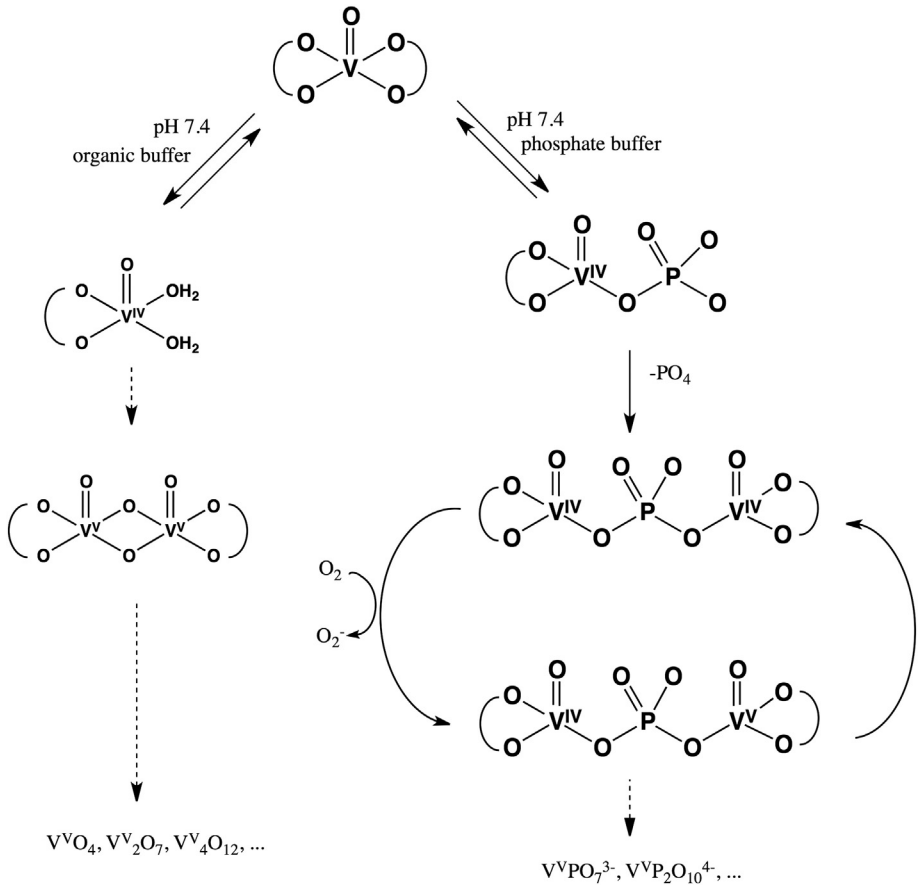

Fig. 12. Proposed pathways for the degradation of $V^{IV}O(acac)_2$ - type complexes in the presence of an organic buffer or phosphate, with generation of superoxide anion.

described for many published vanadium and copper nucleases in organic buffers [1]. While it creates a concern on the use of VC as therapeutic drugs, this knowledge may also be used in the design of new complexes: on the one hand, searching for compounds that take advantage of the interaction with phosphate to generate ROS for the treatment of cancer; on the other hand, searching for vanadium based pharmaceuticals that cannot form vanadium–phosphate species and, hence, are safer.

Abbreviations

acac	2,4-pentanedione, also called acetylacetone
AGE	agarose gel electrophoresis
bPO_4	phosphate buffer
Cl-acac	3-chloro-2,4-pentanedione
CV	cyclic voltammetry
Et-acac	3-ethyl-2,4-penthanedione
Hd	3,5-hepthanedione
HEPES	4-(2-hydroxyethyl)-1-piperazineethanesulfonic acid
Lin	linear form of pDNA
Me-acac	3-methyl-2,4-penthanedione
MOPS	3-(N-morpholino)propanesulfonic acid
MPA	mercaptopropionic acid
Nck	open circular form of pDNA
Oxone	active oxygen (potassium peroxomonosulfate compound)
PBS	phosphate buffered saline
pDNA	plasmid DNA
phen	1,10-phenanthroline
ri	molar ratio of metal per DNA base pairs
ROS	reactive oxygen species
Sc	supercoiled form of pDNA
SCE	saturated calomel electrode
SWV	square wave voltammetry
UV–Vis	UV–visible
VC(s)	vanadium complex(es)

Acknowledgments

The authors gratefully acknowledge the financial support from FEDER and Fundação para a Ciência e Tecnologia (SFRH/BPD/34695/2007, PEst-OE/QUI/UI0100/2013 and Investigador FCT), the IST-UTL Centers of the Portuguese NMR and Mass Spectrometry Networks (REM2013, RNNMR), RECI/QEQ-QIN/0189/2012, RECI/QEQ-MED/0330/2012). N. Butenko is thankful to Fundação para a Ciência e Tecnologia (SFRH/BD/69444/2010) and the Erasmus Mundus External Cooperation Window – Lot 6 for the PhD grants.

Appendix A. Supplementary material

Supplementary data to this article can be found online at http://dx.doi.org/10.1016/j.jinorgbio.2015.04.010.

References

[1] N. Butenko, A.I. Tomaz, O. Nouri, E. Escribano, V. Moreno, S. Gama, V. Ribeiro, J.P. Telo, J. Costa Pesssoa, I. Cavaco, J. Inorg. Biochem. 103 (2009) 622–632.
[2] A.K. Srivastava, M.Z. Mehdi, Diabet. Med. 22 (2005) 2–13.
[3] K.H. Thompson, C. Orvig, J. Inorg. Biochem. 100 (2006) 1925–1935.
[4] K.H. Thompson, J. Lichter, C. LeBel, M.C. Scaife, J.H. MacNeill, C. Orvig, J. Inorg. Biochem. 103 (2009) 554–558.
[5] M.W. Makinen, M. Salehitazangi, Coord. Chem. Rev. 279 (2014) 1–22.
[6] J.C. Pessoa, S. Etcheverry, D. Gambino, Coord. Chem. Rev. (2015)http://dx.doi.org/10.1016/j.ccr.2014.12.002 (In press, Corrected Proof).
[7] L. Pettersson, I. Andersson, A. Gorzsas, Coord. Chem. Rev. 237 (2003) 77–87.
[8] A. Gorzsas, I. Andersson, L. Pettersson, J. Inorg. Biochem. 103 (2009) 517–526.
[9] T. Kiss, E. Kiss, E. Garribba, H. Sakurai, J. Inorg. Biochem. 80 (2000) 65–73.

[10] T. Kiss, E. Kiss, G. Micera, D. Sanna, Inorg. Chim. Acta 283 (1998) 202–210.
[11] T. Jakusch, J. Costa Pessoa, T. Kiss, Coord. Chem. Rev. 255 (2011) 2218–2226.
[12] D.C. Crans, M.L. Tarlton, C.C. McLauchlan, Eur. J. Inorg. Chem. (2014) 4450–4468.
[13] D.C. Crans, J.J. Smee, E. Gaidamauskas, L. Yang, Chem. Rev. 104 (2004) 849–902.
[14] C.C. McLauchlan, Benjamin J. Peters, Gail R. Willsky, Debbie C. Crans, Coord. Chem. Rev. (2015)http://dx.doi.org/10.1016/j.ccr.2014.12.012.
[15] W.R. Harris, Clin. Chem. 38 (1992) 1809–1818.
[16] J. Costa Pessoa, I. Tomaz, Curr. Med. Chem. 17 (2010) 3701–3738.
[17] E.B. Cady, D.A. Jones, J. Lynn, D.J. Newham, J. Physiol. 418 (1989) 311–325.
[18] I. Nadersson, A. Gorzas, C. Kerezsi, I. Toth, L. Pettersson, Dalton Trans. (2005) 3658–3666.
[19] J. Costa Pessoa, I. Cavaco, I. Correia, I. Tomaz, P. Adão, I. Vale, V. Ribeiro, M.M.C.A. Castro, C.C.F.G. Geraldes, in: K. Kustin, J. Costa Pessoa, D.C. Crans (Eds.), Vanadium: The Versatile Metal, ACS Symposium Series, vol. 974, American Chemical Society 2007, pp. 340–351.
[20] M. Mahroof-Tahir, D. Brezina, N. Fatima, M. Iqbal Choudhary, Atta-ur-Rahman, J. Inorg. Biochem. 99 (2005) 589–599.
[21] S.S. Amin, K. Cryer, B. Zhang, S.K. Dutta, S.S. Eaton, O.P. Anderson, S.M. Miller, B.A. Reul, S.M. Brichard, D.C. Crans, J. Inorg. Chem. 39 (2000) 406–416.
[22] A. Doadrio, A.G. Carro, An. R. Soc. Esp. Fis. Quim. 60 (1964) 495–504.
[23] M.B. Fisher, S.J. Thompson, V. Ribeiro, M.C. Lechner, A. Rettie, Arch. Biochem. Biophys. 356 (1998) 63–70.
[24] J. Bernardou, G. Pratviel, F. Bennis, M. Girardet, B. Meunier, Biochemistry (1989) 7268–7275.
[25] S. Nigam, Validation of methods for measuring efficiency of inorganic nucleases(MSc Thesis) European Master in Quality in Analytical Laboratories, University of Algarve, Faro, Portugal, 2011.
[26] M. Saran, K.H. Summer, Free Radic. Res. 31 (1999) 429–436.
[27] N. Steens, A.M. Ramadan, G. Absillis, T.N. Parac-Vogt, Dalton Trans. 39 (2010) 585–592.
[28] G. Verquin, G. Fontaine, M. Bria, E. Zhilinskaya, E. Abi-Aad, A. Aboukais, B. Baldeyrou, C. Bailly, J.-L. Bernier, J. Biol. Inorg. Chem. 9 (2004) 345–353.
[29] L.F. Vilas Boas, J. Costa Pessoa, in: G. Wilkinson, R.D. Gillard, J.A. Mc Cleverty (Eds.), Comprehensive Coordination Chemistry, vol. 3, Pergamon, Oxford 1987, pp. 453–583.
[30] J. Costa Pessoa, L.F. Vilas Boas, R.D. Gillard, R. Lancashire, Polyhedron 7 (1988) 1245–1262.
[31] E. Garribba, G. Micera, D. Sanna, Inorg. Chim. Acta 359 (2006) 4470–4476.
[32] D. Mustafi, M.W. Makinen, Inorg. Chem. 46 (2005) 5580–5590.
[33] D.C. Crans, A.R. Khan, M. Mahroof-Tahir, S. Mondal, S.M. Miller, A. Cour, O.P. Anderson, T. Jakusch, T. Kiss, J. Chem. Soc. Dalton Trans. (2001) 3337–3345.
[34] D. Crans, J. Inorg. Biochem. 80 (2000) 123–131.
[35] D. Rehder, J. Costa Pessoa, C.F.G.C. Geraldes, M. Margarida, C.A. Castro, T. Kabanos, T. Kiss, B. Meier, G. Micera, L. Pettersson, M. Rangel, A. Salifoglou, I. Turel, D. Wang, J. Biol. Inorg. Chem. 7 (2002) 384–396.
[36] C.J. Ballhausen, H.B. Gray, Inorg. Chem. 1 (1962) 111–122.
[37] G.R. Hanson, Y. Sun, C. Orvig, Inorg. Chem. 35 (1996) 6507–6512.
[38] A.J. Bard, L.R. Faulkner, Electrochemical Methods Fundamentals and Applications, John Wiley & Sons Inc. (WIE), New York, 1980.
[39] J.C. Helfrick, J. Lawrence, A. Bottomley, Anal. Chem. 81 (2009) 9041–9047.
[40] L. Linxiang, Y. Abe, Y. Nagasawa, R. Kudo, N. Usui, K. Imai, T. Mashino, M. Mochizuki, N. Miyata, Biomed. Chromatogr. 18 (2004) 470–474.
[41] W. Freinbichler, L. Bianchi, M.A. Colivicchi, C. Ballini, K.F. Tipton, W. Linert, L.D. Corte, J. Inorg. Biochem. 102 (2008) 1329–1333.
[42] T.J. Mason, J.P. Lorimer, D.M. Bates, Y. Zhao, Ultrason. Sonochem. (1994) S91–S95.
[43] J.C. Barreto, G.S. Smith, N.H. Strobel, P.A. McQuillin, T.A. Miller, Life Sci. 56 (1995) (PL-89–PL-96).
[44] E.B. Yan, J.K. Unthank, M. Castillo-Melendez, S.L. Miller, S.J. Langford, D.W. Walker, J. Appl. Physiol. 98 (2005) 2304–2310.
[45] V.M. Mishin, P.E. Thomas, Biochem. Pharmacol. 68 (2004) 747–752.
[46] G.D. Dai, L.B. Cui, L. Song, R.Z. Zhao, J.F. Chen, Y.B. Wang, H.C. Chang, X.R. Wang, Biomed. Environ. Sci. 19 (2006) 8–14.
[47] W. Freinbichler, M.A. Colivicchi, C. Stefanini, L. Bianchi, C. Ballini, B. Misini, P. Weinberger, W. Linert, D. Vareslija, K.F. Tipton, L.D. Corte, Cell. Mol. Life Sci. 68 (2011) 2067–2079.
[48] B. Halliwell, J.M.C. Gutteridge, Free Radicals in Biology and Medicine, Fourth ed. Oxford University Press, Oxford, 2007.
[49] M. Saran, C. Michel, K. Stettmaier, W. Bors, Free Radic. Res. 33 (2000) 567–579.
[50] L.A. Reinke, J.M. Rau, P.B. MacCay, Free Radic. Biol. Med. 16 (1994) 485–492.
[51] S.I. Liochev, I. Fridovich, Arch. Biochem. Biophys. 279 (1990) 1–7.
[52] J.W. Larson, J. Chem. Eng. Data 40 (1995) 1276–1280.
[53] D. Rehder, Bioinorganic Vanadium Chemistry, John Wiley & Sons, New York, 2008.
[54] N. Steens, A.M. Ramadan, T.N. Parac-Vogt, Chem. Commun. (2009) 965–967.
[55] D.C. Crans, A.M. Trujillo, P.S. Pharazyn, M.D. Cohen, Coord. Chem. Rev. 255 (2011) 2178–2192.

Please cite this article as: N. Butenko, et al., The effect of phosphate on the nuclease activity of vanadium compounds, J. Inorg. Biochem. (2015), http://dx.doi.org/10.1016/j.jinorgbio.2015.04.010